Synthetic Scene Generation of the Stennis V&V Target Range for the Calibration of Remote Sensing Systems

Changyong Cao, Slawomir Blonski, Robert Ryan, and Jerry Gasser

Lockheed Martin Stennis Operations
Stennis Space Center, MS 39529

Vicki Zanoni

NASA CRSP Program Office
Stennis Space Center, MS 39529

Synthetic Scene Generation of the Stennis V&V Target Range for the Calibration of Remote Sensing Systems[*]

Changyong Cao, Slawomir Blonski, Robert Ryan, and Jerry Gasser
Lockheed Martin Stennis Operations
Stennis Space Center, MS 39529

Vicki Zanoni
NASA CRSP Program Office
Stennis Space Center, MS 39529

ABSTRACT

The verification and validation (V&V) target range developed at Stennis Space Center is a useful test site for the calibration of remote sensing systems. In this paper, we present a simple algorithm for generating synthetic radiance scenes or digital models of this target range. The radiation propagation for the target in the solar reflective and thermal infrared spectral regions is modeled using the atmospheric radiative transfer code MODTRAN 4. The at-sensor, in-band radiance and spectral radiance for a given sensor at a given altitude is predicted. Software is developed to generate scenes with different spatial and spectral resolutions using the simulated at-sensor radiance values.

The radiometric accuracy of the simulation is evaluated by comparing simulated with AVIRIS acquired radiance values. The results show that in general there is a good match between AVIRIS sensor measured and MODTRAN predicted radiance values for the target despite the fact that some anomalies exist. Synthetic scenes provide a cost-effective way for in-flight validation of the spatial and radiometric accuracy of the data. Other applications include mission planning, sensor simulation, and trade-off analysis in sensor design.

Key words: synthetic scene, radiance, target, simulation.

I. INTRODUCTION

A verification and validation (V&V) target range has been built at Stennis Space Center in an effort to support the in-flight calibration of remote sensing systems. Since the target range became operational in early 1998, several airborne systems have acquired images over the target for performance verifications. These systems included Jet Propulsion Laboratory's (JPL's) Advanced Visible Infrared Imaging Spectrometer (AVIRIS), NASA Stennis' Airborne Terrestrial Applications System (ATLAS), and ADAR 5500 system by Positive Systems, Inc. Preliminary test flights suggest that the target range is very useful for sensor performance verifications. They also raise some issues in determining the optimum flight angle, and flight altitude in relation to the instantaneous field of view (IFOV). In addition, the at-sensor radiance values of the target scene at a given altitude are often unknown, which makes it difficult to verify the radiometric accuracy of the sensor being tested.

In this paper we present an algorithm that allows users to create synthetic scenes or digital models of the Stennis target range with simulated at-sensor radiance values. The software allows users to simulate the scene for their mission before the actual flight. Users can perform trade-off studies on a number of variables including IFOV and ground sample distance (GSD), solar and view geometry, and atmospheric effects. The intent is to allow users to simulate the imagery product before an actual flight mission, which should make missions more

successful and result in savings in both time and effort.

There are different approaches in developing radiance scenes. One approach resamples existing images acquired by sensors with a higher resolution, another approach, or the physics-based approach, uses radiation propagation models and reflectance/emissivity materials maps developed based on specifications and spectral libraries. For the first approach, the derived at-sensor radiances are transient radiance values, which depend on the time, place, and atmospheric conditions for a specific mission. Besides, it is often difficult to remove both the spatial and radiometric sensor artifacts of the system used in image acquisition. Therefore, it is believed that the physics-based approach provides a better solution for high fidelity simulations. This approach becomes even more attractive as the computing speed of desktop computers increases, reducing the time required to perform computational intensive radiation propagation modeling. Some commercially available software packages use the physics-based approach and can probably be used to generate the Stennis target scene once the data base is developed and imported to their software package. However, to the general public, this type of package is not readily available. The simple algorithm presented in this paper uses the physics-based approach, along with a computer program developed in object-oriented C++. Results from Moderate Resolution Transmittance Code (MODTRAN) (Acharya, et al, 1998), among other parameters, are used to generate synthetic at-sensor radiance scenes of the Stennis target range.

Target Specifications

The Stennis target range is built on a landfill near the north gate inside the Stennis Space Center. The center coordinate of this target is at latitude 30.3867 north, and longitude 89.6278 west. The target occupies a flat area of 150x150 square meters and it is painted on concrete with special paints that have the desired spectral reflectance properties.

With a true north-south orientation, the target can be divided into two sections (Figure 1). The west section (left side) is made of black and white rectangular panels and is useful for measuring the modulation transfer function (MTF) and the spatial resolution of the sensor under testing. The east section (right side) is made of four smaller rectangular gray panels that are named 13%, 20%, 30%, and 40% gray panels. The percentage here supposedly represents the reflectance of the paint but

as it is discussed below, the actual spectral reflectance of the paint must be in-situ measured. The gray panels are used for the radiometric verification of sensors. Spaces are also reserved on the east side for deployable and future hyperspectral targets.

Figure 1. Stennis Verification and Validation Target Range

The nominal percent reflectance of a panel is useful only for panel identification purpose. This is because the actual reflectance is a function of a number of parameters. First of all, the spectral reflectance of the paint is not a constant (Figure 2). For example, the 40% gray panel has a reflectance of 20% at the wavelength 0.38 µm and it increases sharply to
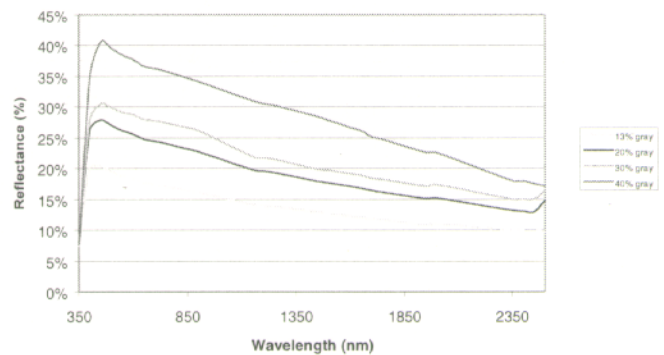

Figure 2. Spectral Reflectance of the Gray Panels on the Target

41% at wavelength 0.42µm. Then it gradually decreases to 20% at wavelength 2.2µm. Secondly, the reflectance of the paint could be a function of time. When the panels were initially painted, the paint was fresh and clean. As time goes by, the paint

may gradually fade and the reflectance values are expected to change.

The spectral reflectances of the panels are used in at-sensor radiance simulations. Therefore, they should be measured on or near the date of the overflight. The Stennis ground data collection team frequently measures the reflectance of the panels and may be contacted for more information.

The local climate and related environmental characteristics play an important role in at-sensor radiance simulations. Stennis is located inside the Hancock county, Mississippi, where the long summers are hot and humid. In summer the average temperature is 81 °F, and the average daily maximum temperature is 89 °F. In winter the average temperature is 52 °F, and the average daily minimum temperature is 43 °F. The hot temperature may contribute a great deal to the at-sensor radiance in the thermal infrared spectral region. The total annual precipitation is about 56 inches, of which 55% usually falls in April through September. The average relative humidity in the mid-afternoon is around 60%. Humidity is higher at night, and the average at dawn is about 90% (SCS, 1981).

Humidity is a dominating factor for the water absorption depth in the spectral radiance simulations. In fact, because of the effect of water vapor, inflight radiometric calibration is often conducted in desert areas where it is relatively dry. Water vapor also contributes to scattering, which increases uncertainties in the scattered radiance. Another factor is the cloudiness, which has a major impact on the at-sensor radiance. When it is cloudy, there is more scattered light and less reflected light, which reduces the contrast in the target radiance scenes. In summer, 65% of the time are sunny days and it decreases to 50% in the winter. In the summer, the weather changes more frequently. Afternoon showers are common and the dynamics of the clouds have a significant impact on the radiance measurements.

According to the soil map(SCS, 1981), the Stennis target is in an area that is nearly level to gently sloping, with moderately well drained to poorly drained silty and loamy soils. It is clear that this sub-tropic environment makes radiometric verification a rather challenging task.

II. AT-SENSOR RADIANCE SIMULATIONS

Currently, most of the optical remote sensing instruments are designed to detect the electromagnetic energy in two main spectral regions: the reflective spectral region which covers from 0.4 to 2.5 μm, and the thermal infrared spectral region which is from 3.0-15 μm. The Stennis target is mainly built for the verification of reflective remote sensing instruments, although it could partially be used for thermal verification. For remote sensing in the 0.4 – 2.5 μm spectral region, sensors are designed to detect the reflected radiance, which is affected by a large number of parameters. Some of the parameters include the solar and view geometry, spectral reflectance of the ground material under observation, surface orientation and bi-directional reflectance properties, and atmospheric scattering and absorption. A simplified version of the governing equation for the at-sensor radiance can be expressed as follows (PRA, 1998):

$$L_{sensor} = L_{solar} * \rho_{BRDF} * cos(z) + L_{sky} * \rho_{diffuse} + L_{bb}(T) * \varepsilon * \tau_{path} + L_{path}$$

Where:

L_{sensor}: at sensor radiance
$(W/m2*sr*\mu m)$
L_{solar}: direct solar irradiance
$(W/cm2*\mu m)$
ρ_{BRDF}: target bidirectional reflectance.
$cos(z)$: cosine of the solar zenith angle
L_{sky}: Diffuse skyshine
$\rho_{diffuse}$: diffuse reflectance
L_{bb}: blackbody radiance
T: target temperature
ε: target emissivity
τ_{path}: path transmittance
L_{path}: path radiance

However, predicting the at-sensor radiance, given a set of parameters, is not a trivial task and it is often done using atmospheric radiative transfer codes. One of the commonly used atmospheric radiative transfer codes is MODTRAN (version 4), which has been widely used for various simulations involving the atmosphere. The latest versions of MODTRAN also allow the user to specify the surface spectral reflectance for a specific material as well as the spectral response of the sensor so that the at-sensor radiance simulation can be done in one step. In our study, MODTRAN 4 is used for generating the at-sensor radiance of the different panels on the target range.

Several groups of parameters in MODTRAN should be carefully chosen for a specific simulation to generate meaningful results. The following variables are especially important for simulating at-sensor radiance: 1) The surface spectral reflectance of a material is a determining factor for the reflected radiance from the ground material. The higher the reflectance of the surface material, the higher the reflected radiance will be. 2) For remote sensing, the view geometry is normally specified as looking straight down from the platform. Therefore, in MODTRAN simulations, the view zenith angle for nadir viewing is specified as 180 degrees. 3) The sensor altitude and ground elevation affect the amount of path radiance in the simulation, which could be significant especially in low visibility for low reflectance targets. 4) The normalized sensor spectral response is used in computing the in-band radiance and average spectral radiance values for a given sensor and should be specified in the filter file. 5) Finally, there are several options to specify the solar geometry. One option is to specify the latitude and longitude of the location and the time and use MODTRAN to compute the solar geometry. Another option is to indicate the position of the Sun using solar zenith and azimuth angles. These angles can be derived from other software packages such as Satellite Toolkit (STK) (AGI, 1998) by specifying the date, time, location, ground elevation, and sensor altitude. We found that the second approach gives us a better control on the angular values in the simulation. In addition, STK provides a graphic display of the simulation scenario.

The total, reflected, and scattered radiance values can be obtained from MODTRAN output. The total radiance (unit: W/cm2*um*sr) is a combination of both the ground reflected and path radiances that reach the sensor. If the sensor spectral response filter is used, MODTRAN automatically generates a *.chn* file in which the in-band radiance and average spectral radiance for each band is produced.

In earlier versions of MODTRAN, computing the in-band radiance had to be done separately as follows: MODTRAN simulations produce the spectral radiance that covers a continuous spectral region at a specified resolution(up to 2 cm^{-1}). For a given sensor, it is only sensitive to a narrow spectral region. Therefore, for a given band, the total amount of energy (or in-band radiance) that the sensor receives can be computed as follows:

$$L \text{ in-band} = \int_{\lambda 1}^{\lambda 2} L(\lambda 1) * R(\lambda) \, d\lambda$$

where:

    $L(\lambda)$: The at-sensor spectral radiance computed in MODTRAN(W/cm2*μm*sr).

    $R(\lambda)$: Sensor spectral response (normalized to 1.0). Unitless.

    $\lambda 1$: The lower wavelength limit that the sensor is responsive to. Unit: μm.

    $\lambda 2$: The upper wavelength limit that the sensor is responsive to. Unit: μm

    L in-band: The in-band radiance for a specific band. Unit: W/cm2*sr.

As a result, for each simulation, one in-band radiance value is produced for each band and each uniform area on the target. For example, to simulate a scene with one band for the target range, seven in-band radiance values are produced, one for each panel on the target range.

III. TARGET MODEL GENERATION -- THE ALGORITHM

After the in-band radiance values are computed, these values are used as input for generating the target radiance scene using a C++ computer program. One major consideration in generating the target scene is that the program has to be flexible enough to generate scenes with different ground sample distances (GSD). This is because in simulating images with different resolutions, one must start with an input scene that has a much finer GSD than the output image. For example, to simulate a 1-meter resolution image, a 10-cm GSD input scene is preferred to simulate the various Modulation Transfer Functions (MTF) effects properly. The algorithm introduced here uses an object-oriented design as described below:

In object-oriented programming, an important step is the object design. Objects are defined at high levels of abstractions. Each object has properties and methods. For the target range, the fundamental abstract object is a rectangle. In other words, the edge target is made of rectangles. These rectangles have the following properties: the starting (x1,x2), and ending location (y1,y2) relative to the origin of the edge target (which is defined as the upper left corner in our study), and the in-band radiance values computed in the previous step. The within (int x, int y) function is designed to determine whether a point

(x,y) falls inside the current rectangle. The ratio (float x) method allows us to calculate the position of x in the target, which makes it flexible to handle scenes with various GSD's. The width() and height() functions return the width and height of the current panel. The prototypical definition of the rectangle object is as follows.

```
class Target
{
public:
        float value;
        int x1,x2,y1,y2;
        int width() {return abs(x2-x1);}
        int height(){return abs(y2-y1);}

        BOOL within(int x,int y)
        {
                if ((x>=x1)&&(x<=x2)&&
                (y>=y1)&&(y<=y2))
                        return TRUE;
                else return FALSE;

        }
        float ratio(float x) {
        return (x/TargetSize);}
};
```

Using this approach, each of the panels on the target is an object of Target with different values and positional parameters. For example, we define the different pads as class gray13, gray20, gray30, gray40, black, and white. Each of these pads has properties (at-sensor radiance values) and methods. The in-band radiance values of the panels are read in from an external file (.chn) which is generated by MODTRAN 4.

IV. MODEL VALIDATION

A major concern in any simulation work is the validity of the simulated products. To validate the model, we compare model generated at-sensor radiance values with the quasi-standard AVIRIS measured radiance values. We found that although there are some differences for the dark and white panels, in general the model predicted values matched the AVIRIS measured at-sensor radiance values. The validation process is described in the following section.

Aviris Overflight Of The Stennis Target Range

The overflight of the Stennis target range took place on October 27, 1998. There were five flightlines covering the target range and the main building complex onsite. The time was from 16 11 50 GMT

to 16 47 10 GMT. The Twin Otter airplane flew at two different altitudes: 2200 meters and 4000 meters, which allowed AVIRIS to acquire images with resolutions of 2.2 and 4 meters, respectively. The AVIRIS images were calibrated to radiance images and then geo-rectified at JPL. Figure 3 shows a sample image with 2.2-meter GSD. It is observed from the image that some target panels appear to be non-uniform mainly due to target contamination. To extract spectra from a uniform area on a panel, principal component analysis is applied to the target image. The result is a PCA image with 224 components. Based on the PCA analysis, pixels from relatively uniform areas on the panels are extracted.
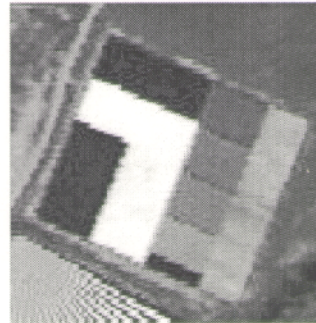

Figure 3. AVIRIS overflight of the Stennis V&V target (bands: R:50,G:38,B:15)

At the same time of the AVIRIS overflight, the Stennis ground data collection team collected ground spectral reflectance for the various panels of the target. A radiosonde was also launched to collect the temperature, humidity, and pressure at various altitudes.

Simulations Using MODTRAN

The objective is to simulate the at-sensor radiance based on the scenario for the AVIRIS mission. The input parameters include the geographic location at 30.3867 (lat) and 89.6378 (longitude), 2200-meter altitude, October 27, 1998, 16.02 GMT, and mid-latitude summer. Since there was no measurement on the optical depth, we had to experiment with various visibilities to empirically determine this value. The results suggest that the 100-km visibility produced results that matched relatively well over the entire spectral range.

It is found that while the simulated spectral radiance curve matched relatively well with the AVIRIS acquired spectral radiance curve (Figure 4), there are some anomalies as well. The problem is that there appears to be a gap in either the visible or the near

infrared spectral region, depending on the visibility used in the simulation. This gap is small for the white panel but increases as the panel reflectance decreases. It is also found that for the black panel, the scattered radiance becomes dominant compared to the reflected radiance. Therefore, it is believed that the discrepancies are probably caused by the biases in modeling and quantifying scattered radiance.
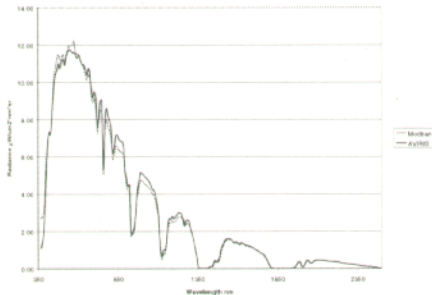

Figure 4. AVIRIS vs. Modtran Simulated Radiance for the Gray 40% Panel Mid-latitude Summer, 100km visibility

Comparisons with Other Models

The atmospheric removal code ATREM (ATmosphere REMoval Program) (CSES 1999) was used in retrieving the surface reflectance from the AVIRIS radiance image. This allowed us to compare the ground measured reflectance curve with the AVIRIS derived reflectance curve. The ATREM result suggests that for the black panel, there is a gradual increase in the reflectance spectrally. This result is consistent with the result from MODTRAN where the simulated radiance is relatively higher in the near-infrared spectral region than in the visible region.

The atmospheric transfer code 6S (Second Simulation of the Satellite Signal in the Solar Spectrum) (Vermote, 1997) is also used in our simulation for cross verification. The simulated apparent reflectance is converted to apparent radiance and compared to results from MODTRAN. The results show that 6S and MODTRAN produced consistent results.

An Example

A sample synthetic scene with a 10 cm GSD is generated using the software introduced above (Figure 5). The scene represents the in-band at-sensor radiance for AVIRIS bands 126, 42, and 19. The in-band radiance values are simulated in MODTRAN using the following parameters: latitude 30.3867°,

longitude 89.6378°, altitude 2.2 km, on October 27, 1998, 16.02 GMT, and mid latitude summer. The MODTRAN simulation covered a spectral range from 0.4µm to 2.5 µm. Using the AVIRIS spectral response, MODTRAN automatically generated the in-band radiance value for these bands in the .chn file.
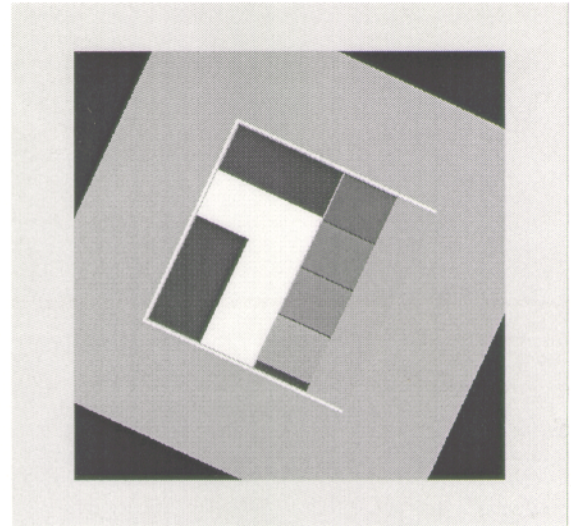

Figure 5. Simulated AVIRIS (RGB bands: 126, 42, and 19) At-Sensor Radiance Input Scene

The output scene is a RGB composite display of three AVIRIS bands. The image has 1500 rows and 1500 columns with no header. The data type is floating point in Intel byte order (generated on Windows NT). This synthetic scene has been subsequently used in generating simulated AVIRIS images by convolving with the Modulation Transfer Function for the AVIRIS sensor.

Model Limitations

The algorithm presented here uses a simplified approach in simulating the at-sensor radiance. Several effects are not considered in generating scenes. For example, the model assumes nadir view geometry and does not take into account the radiance variations within the field of view. It does not consider the bi-directional reflectance properties of the target. It does not include the adjacency effects that could be significant in low visibility conditions especially for low reflectance targets. Finally, the model is mostly useful for reflective remote sensing because as it is discovered through field measurements; the panels are not Lambertian surfaces in the thermal infrared spectral region.

V. SUMMARY

A simple algorithm is presented to generate synthetic scenes of the Stennis V&V target range. The algorithm is flexible enough to create scenes with various ground sample distances. Atmospheric Radiative Transfer Code MODTRAN is used in generating the in-band radiance values for a given sensor over the target range. The current algorithm only generates scenes with a true north orientation as it is specified in the target design. However, the output scene can be rotated to a desired orientation using a number of software packages to simulate the nadir looking scene based on the flight direction. The current algorithm assumes that the target area is a flat Lambertian surface. Future studies will also examine the bidirectional reflectance factor and the adjacency effects of the various panels on the target.

The algorithm is potentially useful in a variety of remote sensing applications, including trade-off analysis in new target design, preflight simulation in the verification and validation of sensors, as well as flight angle simulation in determining the optimal flight path in image acquisition.

VI. REFERENCES

Acharya, P.K., A. Berk, L.S. Bernstein, M.W. Matthew, et al., 1998. MODTRAN VERSIONS 3.7 and 4.0 USER'S MANUAL

AGI, 1998. STK Training Manual, Analytical Graphics, Inc., Malvern, PA.

CSES, 1999. ATREM Manual, Center for the Study of Earth From Space, University of Colorado, Boulder, CO.

PRA, 1998. GCI Toolkit Manual, San Diego, CA.

SCS, 1981. Soil Survey of Hancock County, Mississippi, USDA Soil Conservation Service.

Vermote, E., D.Tanre et. al., 1997. Second Simulation of the Satellite Signal in the Solar Spectrum User Guide. Department of Geography, University of Maryland.

REPORT DOCUMENTATION PAGE	*Form Approved* *OMB No. 0704-0188*

The public reporting burden for this collection of information is estimated to average 1 hour per response, including the time for reviewing instructions, searching existing data sources, gathering and maintaining the data needed, and completing and reviewing the collection of information. Send comments regarding this burden estimate or any other aspect of this collection of information, including suggestions for reducing this burden, to Department of Defense, Washington Headquarters Services, Directorate for Information Operations and Reports (0704-0188), 1215 Jefferson Davis Highway, Suite 1204, Arlington, VA 22202-4302. Respondents should be aware that notwithstanding any other provision of law, no person shall be subject to any penalty for failing to comply with a collection of information if it does not display a currently valid OMB control number.
PLEASE DO NOT RETURN YOUR FORM TO THE ABOVE ADDRESS.

1. REPORT DATE *(DD-MM-YYYY)*	2. REPORT TYPE	3. DATES COVERED *(From - To)*
01-10-1999		

4. TITLE AND SUBTITLE
Synthetic Scene Generation of Stennis Target Range for the Calibration of Remote Sensing Systems

5a. CONTRACT NUMBER
NAS13-650

5b. GRANT NUMBER

5c. PROGRAM ELEMENT NUMBER

6. AUTHOR(S)
Changyong Cao

5d. PROJECT NUMBER

5e. TASK NUMBER

5f. WORK UNIT NUMBER

7. PERFORMING ORGANIZATION NAME(S) AND ADDRESS(ES)
Lockheed Martin Space Operations

8. PERFORMING ORGANIZATION REPORT NUMBER

SE-1999-09-00023-SSC

9. SPONSORING/MONITORING AGENCY NAME(S) AND ADDRESS(ES)
Earth Science Application Directorate
Commercial Remote Sensing Program Office

10. SPONSORING/MONITOR'S ACRONYM(S)

11. SPONSORING/MONITORING REPORT NUMBER

12. DISTRIBUTION/AVAILABILITY STATEMENT
Publicly Available STI per form 1676

13. SUPPLEMENTARY NOTES
Conference - International Symposium on Spectral Sensing Research

14. ABSTRACT

15. SUBJECT TERMS

16. SECURITY CLASSIFICATION OF:			17. LIMITATION OF ABSTRACT	18. NUMBER OF PAGES	19b. NAME OF RESPONSIBLE PERSON
a. REPORT	b. ABSTRACT	c. THIS PAGE			Changyong Cao
					19b. TELEPHONE NUMBER *(Include area code)*
U	U	U	UU	8	(228) 688-2544

Standard Form 298 (Rev. 8-98)
Prescribed by ANSI Std. Z39-18